European Journal of Cancer 119 (2019) 44–56

Available online at www.sciencedirect.com

ScienceDirect

journal homepage: www.ejcancer.com

Original Research

Machine learning defined diagnostic criteria for differentiating pituitary metastasis from autoimmune hypophysitis in patients undergoing immune checkpoint blockade therapy

Ahmed Mekki [a,b,c], Laurent Dercle [b,d,e,*], Philip Lichtenstein [e], Ghaida Nasser [c], Aurélien Marabelle [f], Stéphane Champiat [f], Emilie Chouzenoux [g], Corinne Balleyguier [a,b], Samy Ammari [a,b]

[a] *Department of Radiology, Gustave Roussy Cancer Campus, Villejuif, France*
[b] *Université Paris-Saclay, Paris, France*
[c] *Department of Neuroradiology, C.H.U Bicêtre AP-HP, Le Kremlin-Bicêtre, France*
[d] *Gustave Roussy, Université Paris-Saclay, Institut National de La Santé et de La Recherche Médicale (INSERM), U1015, Equipe Labellisée Ligue Nationale Contre le Cancer, Villejuif, F-94805, France*
[e] *Department of Radiology, Columbia University Medical Center, NYC, NY, USA*
[f] *Drug Development Department, Gustave Roussy, Villejuif, France*
[g] *Center for Visual Computing, CentraleSupelec, INRIA Saclay, Gif-sur-Yvette, 91190, France*

Received 15 May 2019; accepted 9 June 2019
Available online 12 August 2019

KEYWORDS
CTLA-4;
PD-1;
PD-L1;
Immune-related adverse events;
Hypophisitis;
Machine learning

Abstract ***Purpose:*** New-onset pituitary gland lesions are observed in up to 18% of cancer patients undergoing treatment with immune checkpoint blockers (ICB). We aimed to develop and validate an imaging-based decision-making algorithm for use by the clinician that helps differentiate pituitary metastasis (PM) from ICB-induced autoimmune hypophysitis (HP).
Materials and methods: A systematic search was performed in the MEDLINE and EMBASE databases up to October 2018 to identify studies concerning PM and HP in patients treated with cytotoxic T–lymphocyte–associated protein 4 and programmed cell death (ligand) 1. The reference standard for diagnosis was confirmation by histology or response on follow-up imaging. Patients from included studies were randomly assigned to the training set or the validation set. Using machine learning (random forest tree algorithm) with the most-described six imaging and three clinical features, a multivariable prediction model (the signature) was developed and validated for diagnosing PM. Signature performance was evaluated using area under a receiver operating characteristic curves (AUCs).

* *Corresponding author*: UMR1015, Université Paris Saclay, Gustave Roussy, Villejuif, France.
E-mail addresses: ahmekki@gmail.com (A. Mekki), laurent.dercle@gmail.com (L. Dercle).

https://doi.org/10.1016/j.ejca.2019.06.020

Results: Out of 3174 screened articles, 65 were included totalising 122 patients (HP: 60 pts, PM: 62 pts). Complete radiological data were available in 82 pts (Training: 62 pts, Validation: 20 pts). The signature reached an AUC = 0.91 (0.82, 1.00), $P < 10^{-8}$ in the training set and AUC = 0.94 (0.80, 1.00), P = 0.001 in the validation set. The signature predicted PM in lesions either $\geq$ 2 cm in size or < 2 cm if associated with heterogeneous contrast enhancement and cavernous extension.

Conclusion: An image-based signature was developed with machine learning and validated for differentiating PM from HP. This tool could be used by clinicians for enhanced decision-making in cancer patients undergoing ICB treatment with new-onset, concerning lesions of the pituitary gland.

1. Introduction

Immune checkpoint blockers (ICBs) primarily function by targeting the immunoinhibitory cytotoxic T-lymphocyte–associated protein 4 (CTLA-4), programmed cell death 1 (PD-1) and programmed cell death ligand (PD-L1). These medications have revolutionised the therapeutic landscape across many solid tumours [1–3]. Their superiority over reference treatments was first demonstrated in melanoma [4,5] and have since expanded on to treat numerous other cancer types [6–10]. The importance of these new anti-cancer treatments is attested to by their registration as a 'breakthrough therapy'; they are now a standard of care in many cancer types and are under therapeutic trial for many others [11]. As a result, their use is no longer limited to the hospitals involved in clinical trials, and they are prescribed in a much wider range of clinical oncology settings across the world. The number of patients exposed to these new therapies is likely to dramatically increase in the near future.

These new immunotherapies, however, bring new challenges for the oncologist. They generate atypical patterns of tumour responses and progression [12–16] as well as unique toxicity profiles [17]. The recognition and management of immune-related adverse events (irAEs) poses new difficulties in particular for imaging physicians. Although still primordial, medical imaging is a cornerstone in the monitoring of patients undergoing ICB therapy. A previous study exploring this fundamental role showed a 74% imaging-based detection rate of anti-PD1–mediated irAEs [18] with the most frequent complications including interstitial lung disease, thoracic sarcoid-like reaction, thyroiditis, hypophysitis (HP), enterocolitis, pancreatitis, hepatitis, arthritis and tenosynovitis.

HP is a well-known endocrinopathy in patients undergoing ICB therapy. The development of immune-related HP has been more frequently observed with the anti-CTLA-4 agent ipilimumab [19–21] because of the expression of CTLA-4 on normal pituitary cells [22]. Its incidence varies between 0.5% and 18% in a recent review [23] and is dose dependent. When ipilimumab is given in combination with the anti-PD-1 agent nivolumab, the incidence of HP is around 8% [24]. In contrast, HP is less frequent in patients treated with anti-PD-1 or anti-PD-L1 monotherapy [25].

The real difficulty in managing HP however comes not from the treatment itself but rather its accurate recognition and differentiation from pituitary metastasis (PM). An uncommon presentation outside of specialised centres, PM rises much higher on the differential for the physician working at a comprehensive cancer centre. One of the largest historical series examined 500 consecutive autopsies in patients with metastatic disease at Memorial Sloan-Kettering Cancer Center and found an incidence of 3.6% [26], a number which may be set to rise as patients with malignancy continue to live longer and be monitored more closely.

The appearance of a focal anomaly in the pituitary gland of patients undergoing ICB therapy for malignancy poses a continued dilemma for the imaging physician and one that comes up regularly at multidisciplinary meetings. The distinction between HP and PM is one that needs to be made quickly to avoid a potentially devastating delay in management. Clinicobiological data are not very discriminating, and histological confirmation requires invasive neurosurgical management. The place of medical imaging is therefore central in differentiating these two pathologies. In cases where the imaging appearance is equivocal, and the diagnosis remains uncertain; however, a few options exist.

The 'wait and see' strategy consists mainly of empiric treatment with corticosteroids when there is a strong HP presumption. This strategy carries the main advantage of non-invasiveness but also the obvious risk of potentially missing the start of a rapidly progressive metastasis. This in turn risks irreversible damage to the visual pathways and a significantly more difficult neurosurgical management. It can also be a source of anxiety in patients with partial or complete response to these treatments. Proceeding with transsphenoidal neurosurgical treatment in

cases of uncertainty will protect the visual pathways and is most advantageous when the lesion is indeed metastatic, but there can be significant morbidity associated with inadvertently resecting an inflamed but otherwise normal pituitary. A third option consisting of treatment with probabilistic radiotherapy also risks permanent damage to the visual pathways in addition to irreversible hypopituitarism, radionecrosis and damage to the internal carotid arteries.

To date, multiple case reports and series have been published describing ICB-related HP as well as PM, but there is no study comparing these two pathologies. Our objective was to assess whether an image-guided decision-making algorithm can enable the non-invasive diagnosis of suspicious pituitary lesions in patients treated by these new anti-cancer immunotherapies. For this purpose, we have performed a systematic review of literature with the aim of making a machine learning–driven algorithm.

2. Methods

2.1. Search methods

A systematic review of the literature was conducted according to the guidelines outlined in the Preferred Reporting Items for Systematic Reviews and Meta-Analyses (PRISMA) statement [27]. The PUBMED and EMBASE databases were searched up to October 20, 2018. For HP, the search method involved querying for the terms 'hypophysitis', 'auto-immune hypophysitis', 'ipilimumab', 'nivolumab', 'pembrolizumab', 'atezolizumab', 'cytotoxic T-lymphocyte antigen 4', 'CTLA-4', 'programmed cell death 1', 'PD-1', 'programmed cell death ligand 1', 'PD-L1', 'immunotherapy', 'checkpoint inhibitor', 'anti-PD-1', 'anti-PD-L1', 'anti-CTLA-4'. The Boolean operator AND was used to combine terms related to HP and ICB. The Boolean operator OR was used to discriminate the similar terms. For PM, the search method involved querying for the terms 'pituitary metastasis', 'metastatic cancer of the pituitary', 'metastatic carcinoma of the pituitary', 'metastasis' and 'pituitary'. No starting point was defined for article screening.

2.2. Inclusion criteria

For study selection, all search hits were evaluated for eligibility by two reviewers screening title and abstracts. Full-text versions of potentially eligible articles were obtained for further evaluation. The reference lists of the included studies were manually searched to identify other potentially eligible articles. Disagreements between the two reviewers in study selection were resolved by consulting a third reviewer (A.M, S.A., L.D.; radiologists with respectively 4, 10 and 8 years of experience).

Inclusion criteria were (i) articles describing either HP or PM with at least three 'standard' radiological signs (defined as any discriminating radiological sign used in more than 50% of the articles included), (ii) a diagnosis of HP confirmed by regression of the lesion with corticotherapy and/or the reduction or cessation of ICB therapy and (iii) a diagnosis of PM either confirmed histologically or by a non-equivocal metastatic progression on subsequent imaging.

Exclusion criteria were (i) studies that were not published in English, (ii) animal studies, (iii) articles with magnetic resonance imaging that was too old or insufficient quality for our evaluation and (iv) association with a pituitary adenoma, meningioma or primary carcinoma of pituitary.

2.3. Data extraction and analysis

Imaging signs were defined based on the international radiological pituitary reference book [28], on our expertise in oncological neuroimaging and on the features most frequently cited in the included articles. First, we recorded all signs available in the selected studies. Second, we considered signs which were evaluated in more than 50% of the included articles as a relevant radiological sign; the remainder were deemed irrelevant and excluded. Third, in the event of insufficient radiological data (less than three relevant 'standard' radiological signs in a patient), the corresponding author was contacted by email to obtain the necessary radiological information. Fourth, in the absence of feedback from the corresponding author, two radiologists (A.M., S.A.) reinterpreted the available images with missing radiological features without knowledge of outcome, clinical data or clinicopathological features. These data are hierarchised in Table 1a for PM and Table 1b for HP (see Table 4).

2.4. Development and validation of the signature in the training set

2.4.1. Performance of the clinical features, radiological features and of the signature

The primary end-point of this study was to train and validate a signature incorporating both clinical and radiological features to diagnose pituitary metastases. The secondary end-point was to compare the accuracy (95 CI%) of (i) clinical features, (ii) radiological features and (iii) the signature.

2.4.2. Predictors included in the signature

All relevant clinical and imaging variables (see above) were evaluated for their efficacy in predicting whether the pituitary lesion represented either a PM or an autoimmune HP.

Table 1a
Study and patient characteristics for hypophysitis.

Author	Year	Country	n	Cancer type	Age	Modality	Treatment type
Van der Hiel *et al.*	2013	The Netherlands	1	Melanoma	77	PET/CT	Ipilimumab
Blansfield *et al.*	2005	United States	8	Melanoma, RCC	49 (31–61)	MR	Ipilimumab
Albarel *et al.*	2014	France	15	Melanoma	55 (39–80)	MR	Ipilimumab
Araujo *et al.*	2015	Brazil	1	Melanoma	60	MR	Ipilimumab
Carpenter *et al.*	2009	United States	3	Melanoma	53 (44–70)	MR	Ipilimumab
Chang *et al.*	2017	United States	1	Melanoma	77	MR	Ipilimumab + Nivolumab
Chodakiewitz *et al.*	2014	United States	3	Melanoma	58 (45–65)	MR	Ipilimumab
Dillard *et al.*	2009	United States	2	Prostate	59 (50–67)	MR	Ipilimumab
Hassanzadeh *et al.*	2017	United States	1	Melanoma	64	MR	Ipilimumab
Johnson *et al.*	2015	United States	1	Melanoma	60	MR	Ipilimumab
Juszczak *et al.*	2012	United Kingdom	1	Melanoma	54	MR	Ipilimumab
Kaehler *et al.*	2009	United Kingdom	1	Melanoma	60	MR	Ipilimumab
Kanie *et al.*	2017	Japan	2	NSCLC	65 (61–69)	MR	Atezolizumab
Mahzari *et al.*	2015	Canada	4	Melanoma	62 (54–80)	MR	Ipilimumab
Majchel *et al.*	2015	United states	1	Melanoma	31	MR	Ipilimumab
Marlier *et al.*	2014	Belgium	4	Melanoma	62 (31–81)	MR	Ipilimumab
Mekki *et al.*	2018	France	3	NSCLC, RCC	59 (53–65)	MR	Nivolumab
Gunawan *et al.*	2018	Australia	1	Melanoma	52	MR	Ipilimumab + Nivolumab
Ohara *et al.*	2018	Japan	1	Oesophagus (SCC)	63	MR	Nivolumab
Okano *et al.*	2016	Japan	1	Melanoma	50	MR	Nivolumab
Valecha *et al.*	2017	United states	1	SCLC	58	MR	Ipilimumab + Nivolumab
Wachsmann *et al.*	2016	United states	1	Melanoma	62	PET/CT	Ipilimumab
Wallace *et al.*	2018	United states	1	Melanoma	49	MR	Ipilimumab
Arvinder *et al.*	2017	United States	1	Melanoma	34	MR	Ipilimumab
Iqbal *et al.*	2016	United Kingdom	1	Melanoma	65	MR	Ipilimumab

RCC = renal cell carcinoma; NSCLC = non-small cell lung cancer; SCC = squamous cell carcinoma; SCLC = small cell lung cancer; PET = positron-emission tomography; CT = computed tomography.

2.4.3. Candidate signature building

Patients were randomly assigned to either the training set or the validation set using a ratio of 3:1. Patients with incomplete relevant clinical or radiological data sets were excluded from the training and validation of the signature. We developed (training set) and validated (validation set) a multivariable prediction model, *i.e.* the signature, to diagnose PM based on all predictors in the training set. Specifically, the signature outputs the probability of a pituitary lesion being a metastasis. Patients with signature value > 0.5 were classified as positive for high-risk of PM and negative/low-risk otherwise. First, area under a receiver operating characteristic curve (AUC) and receiver operating characteristic (ROC) curves were used to rank non-redundant candidate features. To reduce overfitting, a maximum combination of three informative candidate features was selected based on forward search and feature combination. A random forest tree machine learning algorithm (CRT with pruning and 3-fold cross validation) was used to combine features and generate the optimal candidate classification model, *i.e.* the signature, that achieved the best performance in terms of AUC using three-fold cross-validation.

2.4.4. Validation of the signature

The performance of the optimal signature was tested in the validation set containing patients that were never used for training. There was no difference between development data set and validation data set in terms of setting, eligibility criteria, outcome and predictors. In cases of missing data, patients were excluded from the signature building.

2.4.5. Statistical analysis

Data were presented as frequency with percentages for qualitative variables and as mean with standard deviation for continuous variables. Calculated data with P values < 0.05 were considered as statistically significant. The performance of the machine learning algorithm for diagnosing PM was calculated using a binary classifier system (PM versus HP) and non-parametric AUC. All statistical analyses were performed using SPSS software 24.0 (IBM, Armonk, NY). AUC comparisons for correlated ROC curves were performed using Hanley and McNeil techniques.

3. Results

3.1. Search strategy and study selection

The systematic review through MEDLINE and PUBMED databases yielded 3174 records that met the initial search criteria. Fig. 1 outlines the PRISMA consort flow, duplicates and excluded articles. Ultimately, 65 articles were included of which there were 49 case reports and 16 case series; 25 were in the HP group [18,29–52] and 40 were in the PM group [53–92]. This yielded a total of 122 patients (60 in the HP group and 62 in the PM group) included for 'standard' radiological

Table 1b
Study and patient characteristics for pituitary metastases.

Author	Year	Country	n	Cancer type	Age	Modality
Al-Aridi *et al.*	2013	United States	1	NSCLC	–	MR
Dutta *et al.*	2011	India	4	NSCLC	51 (39–60)	MR
Bhatoe *et al.*	2008	India	1	Medullary thyroid	38	MR
Ersoy *et al.*	2007	Turkey	1	Breast	55	PET/CT
Fridley *et al.*	2011	United States	1	SCLC	56	MR
Goglia *et al.*	2007	Italy	1	NET	69	MR
Golkowski *et al.*	2007	Poland	2	Breast,RCC	49 (46–52)	MR
Gopan *et al.*	2007	United States	5	RCC	60 (51–67)	MR
He *et al.*	2014	United States	1	HCC	49	MR
Kam *et al.*	2015	Australia	1	Breast	63	MR
Karamouzis *et al.*	2003	Greece	1	HCC	59	MR
Ko *et al.*	1994	China	1	Lung	67	MR
Koshiyama *et al.*	1992	Japan	1	RCC	57	MR
Lin *et al.*	2008	China	1	Breast	37	MR
Masui *et al.*	2013	Japan	1	Melanoma	68	MR
Ozturk *et al.*	2013	Turkey	1	Colorectal	46	MR
Peppa *et al.*	2009	Greece	1	Breast	52	MR
Piedra *et al.*	2004	United States	1	Breast	58	MR
Riemenschneider *et al.*	2009	Germany	1	Prostate	64	MR
Siqueira *et al.*	2015	Brazil	1	Lung NE	64	MR
Williams *et al.*	2008	United States	1	Medullary thyroid	23	MR
Ratti *et al.*	2013	Italy	1	Rectal	54	MR
Stovanovic *et al.*	2012	Serbia	1	Papillary thyroid	67	MR
Beckett *et al.*	1998	United Kingdom	1	RCC	56	MR
Moreno-Perez *et al.*	2007	Spain	1	HCC	65	MR
Agarwal *et al.*	2014	India	1	NSCLC	52	PET/CT, MR
Barbaro *et al.*	2012	Italy	2	Papillary thyroid	64 (63–65)	MR
Kurkjianet al	2005	United Kingdom	2	Breast	51 (47–54)	MR
Santarpia *et al.*	2009	United States	1	Medullary thyroid	23	MR
Wendel *et al.*	2017	France	1	RCC	61	MR
Feletti *et al.*	2010	Italy	1	Merkel	65	MR
Kim YH *et al.*	2012	South Korea	1	Breast	65	MR
Chu *et al.*	2016	China	1	Breast	60	MR
Kanayama *et al.*	2005	Japan	1	Thymoma	80	MR
Souza mota *et al.*	2018	Brazil	1	Follicular thyroid	58	MR
Rajput *et al.*	2006	India	1	NSCLC	51	MR
Bisof *et al.*	2008	Croatia	1	RCC	49	MR
Hsiao *et al.*	2011	China	1	NSCLC	56	MR
Lim *et al.*	2015	Singapore	2	Thyroid	58 (50–65)	MR
Castlekirszbaum *et al.*	2018	Australia	12	Breast, oesophagus, NSCLC, SCLC, colorectal, melanoma, plasmocytoma	63 (30–87)	MR

NA = data not available; RCC = renal cell carcinoma; NSCLC = non-small cell lung cancer; SCC = squamous cell carcinoma; SCLC = small cell lung cancer; NET = neuroendocrine tumour, NE = neuroendocrine; HCC = hepatocellular carcinoma; PET = positron-emission tomography; CT = computed tomography.

sign determination. Of these, a further 40 patients were excluded from signature building because of insufficient total radiological data.

3.2. Patients' characteristics

Table 1a,b summarises the patient demographics. The mean age of the patient cohort was 56.9 ± 12 years, with range of 23–87 years. Of the 121 patients whose gender was known, 55 patients (45.5%) were female, and 66 (55.5%) were male.

3.3. Imaging signs selection

Amongst a total of 16 imaging signs that were used in these 122 patients, eight were evaluated in more than

Table 2
Immune-related hypophysitis versus pituitary metastases.

Imaging and clinical features	Hypophysitis	PM
Pituitary enlargement	n = 53/59 (89.%)	n = 62/62 (100%)
Homogenous enhancement	n = 31/49 (63.3%)	n = 8/46 (17.4%)
Heterogenous enhancement	n = 18/49 (36.7%)	n = 38/46 (82.6%)
Increased stalk thickness	n = 29/49 (59.2%)	n = 16/58 (27.6%)
Suprasellar extension	n = 35/59 (59.3%)	n = 57/62 (91.9%)
Cavernous extension	n = 0/59 (0%)	n = 31/61 (50.8%)
Size >2 cm	n = 0/59 (0%)	n = 45/61 (73.8%)
18FDGPET hypermetabolism	n = 2/2 (100%)	n = 2/2 (100%)
Headache	n = 42/60 (70%)	n = 41/61 (67.2%)
Hypopituitarism	n = 56/60 (93.3%)	n = 50/59 (84.7%)
Diabetes insipidus	n = 3/60 (5%)	n = 26/52 (50%)

PM = pituitary metastasis.

Table 3
Sensitivity and accuracy of clinical features and imaging features. The machine learning algorithm was designed to maximise the sensitivity for the detection of pituitary metastases, while maintaining accuracy. The values and 95% confidence intervals listed below demonstrate that the algorithm exceeded the performance of any individual feature.

Performance to differentiate PM from HP	Clinical features (all pts)			Imaging features (all pts)						Signature subset (complete data set)	
	Headache	Hypopituitarism	Diabetes insipidus	Pituitary enlargement	Heterogenous enhancement	Stalk thickened	Cavernous extension	Suprasellar extension	Size >2 cm	Signature	Size >2 cm
Total	121	119	112	121	95	107	120	121	110	82	82
Positive in PM (n)	41	50	26	62	38	16	31	57	45	28	25
Positive in hypophysitis (n)	42	56	3	53	18	29	0	35	0	0	0
Negative in PM (n)	20	9	26	0	8	42	30	5	6	7	10
Negative in hypophysitis (n)	18	4	57	6	31	20	59	24	59	47	47
Sensitivity	0.67 (0.55:0.78)	0.85 (0.73:0.92)	0.50 (0.37:0.63)	1.00 (1.00:1.00)	0.83 (0.72:0.94)	0.28 (0.16:0.39)	0.51 (0.38:0.63)	0.92 (0.85:0.99)	0.88 (0.79:0.97)	0.80 (0.67:0.93)	0.71 (0.56:0.86)
Specificity	0.30 (0.20:0.43)	0.07 (0.02:0.17)	0.95 (0.86:0,99)	0.10 (0.02:0.18)	0.63 (0.50:0.77)	0.41 (0.27:0.55)	1.00 (1.00:1.00)	0.41 (0.28:0.53)	1.00 (1.00:1.00)	1.00 (1.00:1.00)	1.00 (1.00:1.00)
False positive rate	0.70 (0.59:0.81)	0.93 (0.87:0.99)	0.05 (0.00:0.10)	0.90 (0.82:0.98)	0.37 (0.23:0.50)	0.59 (0.45:0.73)	0.00 (0.00:0.00)	0.59 (0.47:0.72)	0.00 (0.00:0.00)	0.00 (0.00:0.00)	0.00 (0.00:0.00)
False negative rate	0.33 (0.21:0.44)	0.15 (0.06:0.24)	0.50 (0.37:0.63)	0.00 (0.00:0.00)	0.17 (0.06:0.029)	0.72 (0.61:0.84)	0.49 (0.37:0.60)	0.08 (0.01:0.18)	0.12 (0.03:0.20)	0.20 (0.07:0.31)	0.28 (0.14:0.40)
Positive predictive value	0.49 (0.39:0.60)	0.47 (0.38:0.57)	0.90 (0.79:1.00)	0.54 (0.45:0.63)	0.68 (0.56:0.80)	0.36 (0.22:0.50)	1.00 (1.00:1.00)	0.62 (0.52:0.72)	1.00 (1.00:1.00)	1.00 (1.00:1.00)	1.00 (1.00:1.00)
Negative predictive value	0.47 (0.32:0.63)	0.31 (0.06:0.60)	0.69 (0.59:0.79)	1.00 (1.00:1.00)	0.79 (0.67:0.92)	0.32 (0.21:0.44)	0.66 (0.56:0.76)	0.83 (0.69:0.97)	0.91 (0.84:0.98)	0.87 (0.78:0.96)	0.82 (0.73:0.92)
Overall accuracy	0.50 (0.42:0.59)	0.50 (0.41:0.59)	0.46 (0.37:0.56)	0.56 (0.47:0.65)	0.73 (0.64:0.82)	0.34 (0.25:0.43)	0.75 (0.67:0.83)	0.67 (0.59:0.75)	0.95 (0.90:0.99)	0.91 (0.85:0.98)	0.88 (0.81:0.95)

PM = pituitary metastasis.

Table 4
Median week of immune-related hypophysitis onset stratified by oncological response to the ICB.

Best overall response	n	Median week (range)
PD	6	12 (6–18)
SD	5	21 (9–56)
PR	10	13.5 (3–34)
CR	4	6 (4–12)
Unknown	35	9 (3–28)
Overall	60	10.5 (3–56)

PD = progressive disease; SD = stable disease; PR = partial response; CR = complete response.

50% of the literature and considered as 'standard' radiological signs. The eight 'standard' radiological signs (with % citation and description variables) were pituitary gland enlargement (99.2%, n = 121/122 pts, enlarged versus not enlarged), contrast enhancement (77.9%, n = 95/122 pts, homogenous versus heterogeneous), pituitary stalk thickness (87%, n = 107/122 pts, increased versus normal), cavernous extension (98.4%, n = 120/122 pts, presence versus absence), suprasellar extension (99%, n = 121/122 pts, presence versus absence) and size (98.4%, n = 120/122 pts, increased versus normal [increased size was a continuous variable that we then empirically divided into two categories: $\geq$ 2 cm versus < 2 cm]). 18F fluorodeoxyglucose (FDG)-positron emission tomography (PET) uptake was also included because of its systematic use in the articles of nuclear medicine (100.0%, n = 4/4 pts, normal versus increased). Eight non-'standard' radiological signs were excluded from our analysis: T1 signal, T2 signal, diffusion signal, posterior lobe signal, lesion epicentre, pituitary stalk deviation, chiasma anomaly and peridural enhancement. All of these signs were reported in less than 10% of the manuscript from the literature.

3.4. Performance of the signature

Complete radiological data were available in 82 pts (Training [T]: 62 pts, Validation [V]: 20 pts). The signature reached an AUC = 0.91 (0.82, 1.00), $P < 10^{-8}$ in the training set and AUC = 0.94 (0.80, 1.00), P = 0.001 in the validation set (Fig. 4). The signature predicted a PM in patients that had either a pituitary lesion $\geq$ 2 cm in size or a lesion < 2 cm that also demonstrated both heterogeneous contrast enhancement and cavernous extension (Fig. 3). Table 3 summarises the sensitivity, specificity, positive predictive value and negative predictive value of all modalities. The signature of size $\geq$ 2 cm was most superior in its specificity; a positive finding was observed exclusively in cases of PM (100%; Training: 22/22 pts, Validation: 16/16 pts).

For lesions < 2 cm, the algorithm found that a heterogeneously enhancing lesion associated with cavernous extension was PM 100% of the time. The algorithm suggests HP for lesions that are less than < 2 cm that either enhance heterogeneously without cavernous extension or enhance homogenously. The categories can be broken down as follows (i) size < 2 cm and homogeneous enhancement (T: 3.3%, V:28.0%); (ii) size < 2 cm and heterogeneous enhancement without cavernous extension (T:40%, V:16.7%); (iii) size < 2 cm and heterogeneous enhancement with cavernous

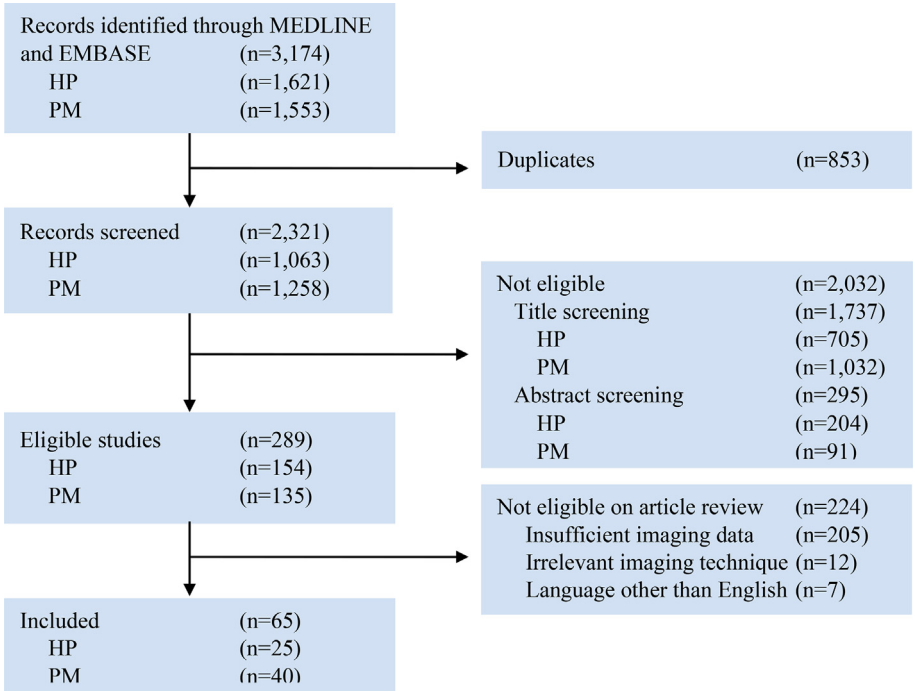

Fig. 1. Study selection flowchart. HP = hypophysitis; PM = pituitary metastasis.

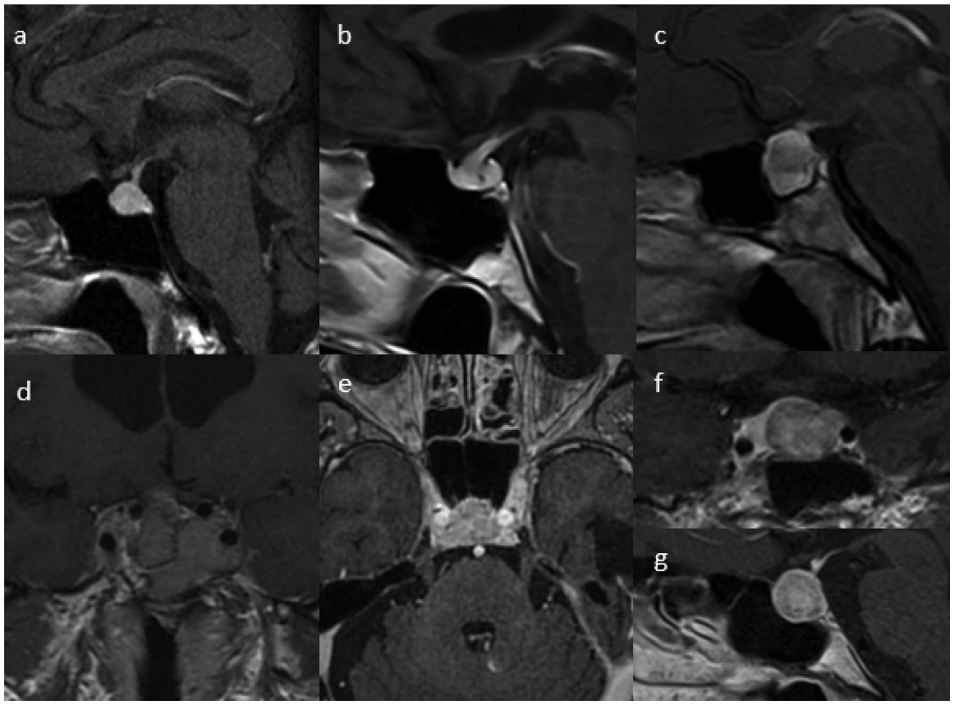

Fig. 2. **Prospective evaluation of the image-driven algorithm.** ICB-induced hypophysitis (a–c) versus pituitary metastases (d–g) on oncological follow-up imaging (post-contrast T1-weighted MRI: sagittal (a, b, c and g), coronal (d and f), and axial (e)). All lesions were correctly predicted as HP or PM by our image-driven algorithm. (a): Enlarged homogenously enhancing pituitary gland with a mildly thickened stalk. (b): Marked thickening of the pituitary stalk. (c): Enlarged pituitary (<2 cm, no cavernous extension) with heterogenous enhancement. (d): Enlarged (≥2 cm, with cavernous extension), heterogeneously enhancing pituitary gland in a patient treated for NSCLC. (e and f-g): Enlarged (<2 cm, with cavernous extension), heterogeneously enhancing pituitary glands in 2 patients treated for RCC. HP = hypophysitis; PM = pituitary metastasis; RCC = renal cell carcinoma; NSCLC = non-small cell lung cancer; MRI = magnetic resonance imaging.

extension (T:100%, V:Not Evaluable) and (iv) size ≥ 2 cm (T: 100%, V:100%)

3.5. Immune-related hypophysitis characteristics

Figs. 2a–c show examples of immune-related HP, and Table 2 summarises immune-related HP disease characteristics by patient. Homogenous enhancement was observed in 63.3% (n = 31/49 pts), and size was never ≥ 2 cm (n = 0/59 pts). The median time of immune-related HP occurrence was 10 weeks (range 3–56 weeks). An objective response to immunotherapy was observed in 56% of patients (n = 14/25 pts), partial response was seen in 40% (n = 10/25 pts), complete response in 16% (n = 4/25 pts), progressive disease in 24% (n = 6/25 pts) and stable disease in 20% (n = 5/25 pts).

3.6. Pituitary metastases characteristics

Figs. 2d–f show examples of pituitary metastases, and Table 2 summarises disease characteristics by patient. Heterogenous enhancement was observed in 82.6% (n = 38/46 pts) and a size ≥ 2 cm in 67.2% (n = 45/61 pts). Primary tumour type was breast in 23% (n = 14/61 pts), non-small cell lung cancer in 18% (n = 11/61 pts), renal cell carcinoma in 16.4% (n = 10/61 pts), thyroid in 13.1% (n = 8/61 pts), hepatocellular carcinoma in 4.9% (3/61 pts), small cell lung cancer in 3.3% (n = 2/61 pts), melanoma in 3.3% (n = 2/61 pts) and other cancer types in 18% (n = 11/61 pts).

4. Discussion

This systematic review of the literature allows us to more accurately characterise the appearance of focal anomalies of the pituitary gland in patients undergoing ICB therapy and differentiate between metastatic progression and an irAE. A radiologic signature achieving the best performance in diagnosing PM was determined using a machine learning–based multivariable prediction model. Additionally, a new methodology was implemented to perform data mining in the existing literature and identify the largest existing cohort of PM and HP. The two most discriminating signs discovered were size ≥ 2 cm and cavernous extension.

The frequency of immune-related HP can reach up to 18% [93], occurs mainly in patients who are responding to immunotherapy and typically appears around 10 weeks after the initiation of treatment. This 10-week delay is a median value with the literature showing a very wide range from 1 to 52 weeks [94]. Although our

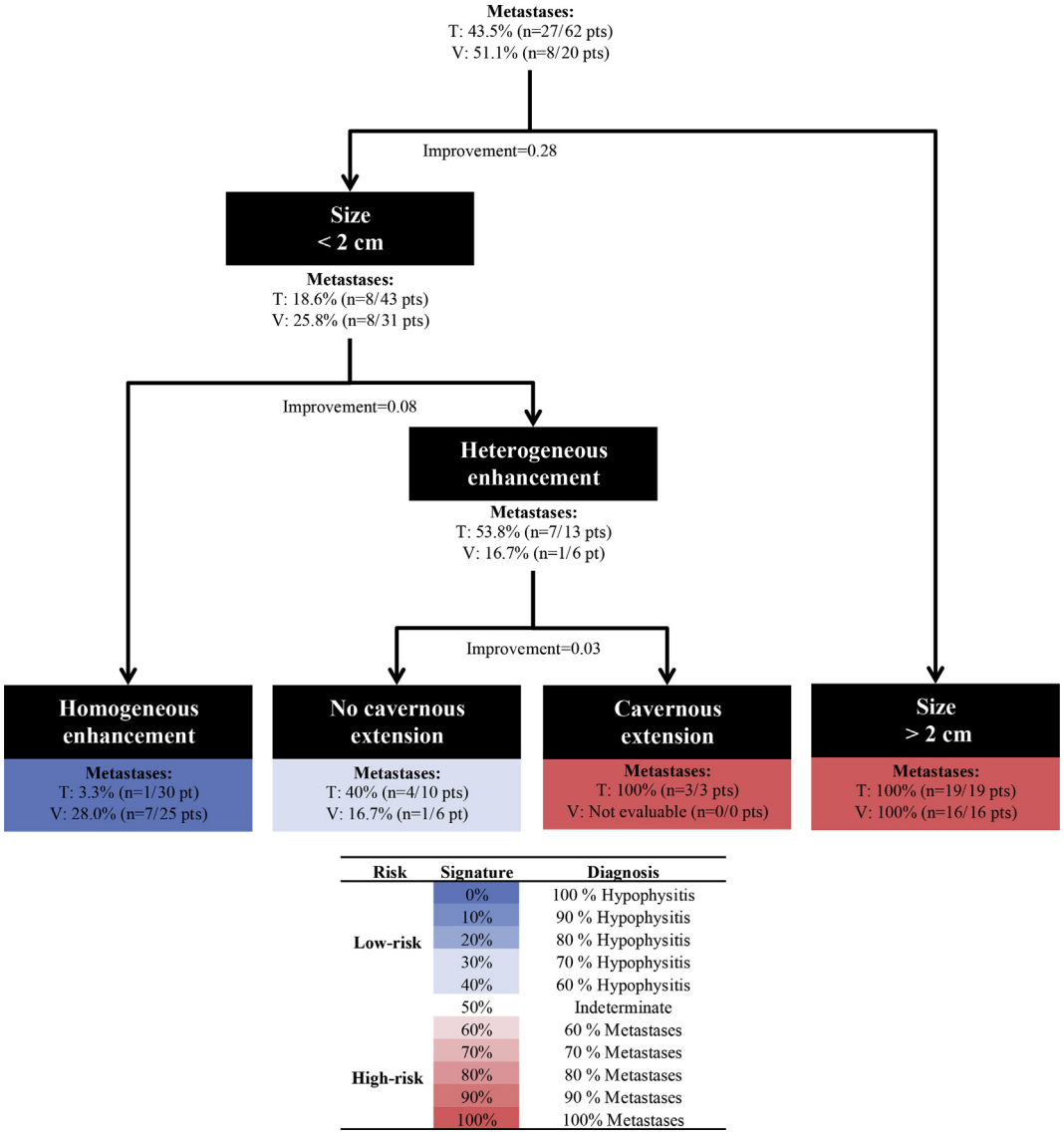

Risk	Signature	Diagnosis
Low-risk	0%	100 % Hypophysitis
	10%	90 % Hypophysitis
	20%	80 % Hypophysitis
	30%	70 % Hypophysitis
	40%	60 % Hypophysitis
	50%	Indeterminate
High-risk	60%	60 % Metastases
	70%	70 % Metastases
	80%	80 % Metastases
	90%	90 % Metastases
	100%	100% Metastases

Fig. 3. **Clinical decision algorithm trained (T) and validated (V) for the diagnosis of hypophysitis versus pituitary metastases.** Four categories were identified: (i) Size<2 cm and homogeneous enhancement (T: 3.3%, V:28.0%); (ii) Size<2 cm and heterogeneous enhancement without cavernous extension (T:40%, V:16.7%); (iii) Size<2 cm and heterogeneous enhancement with cavernous extension (T:100%, V:NE); (iv) Size >2 cm (T: 100%, V:100%).

data mining allowed us to characterise the typical clinic-biological profile of these patients, none of these features were selected by the model. Patients with HP commonly presented with headache and pituitary insufficiency but rarely with diabetes insipidus. The signs and symptoms at diagnosis as well as the pituitary hormone abnormalities largely depend on the degree of pituitary involvement. PM in our review demonstrated the same clinical presentation as HP aside from a higher frequency of diabetes insipidus.

We have seen that the radiological appearance of immune-related HP secondary to ICB therapy is similar to that described in primary HP [28] with diffuse and symmetric enlargement of the pituitary gland as well as frequent suprasellar extension, pituitary stalk thickening and homogenous enhancement. Pituitary metastases also demonstrated enlargement of the pituitary gland, but these often exceeded 2 cm in maximal diameter with frequently extended into the cavernous sinuses (neither of these features were seen in our cohort of HP). An intense, heterogeneous pattern of enhancement also favoured the diagnosis of metastasis.

An important limitation to note is that we have only evaluated the imaging of acute phase HP, when the problem of differentiating from PM is at its greatest. Imaging of the late phase of HP typically poses less of a dilemma as atrophy of the anterior pituitary is common. Moreover, we did not include in our analysis the possibility of pituitary adenoma given the fact that patients will usually have baseline brain imaging, and the occurrence of new pituitary adenomas in an oncological context is unlikely. Finally, several radiological signs

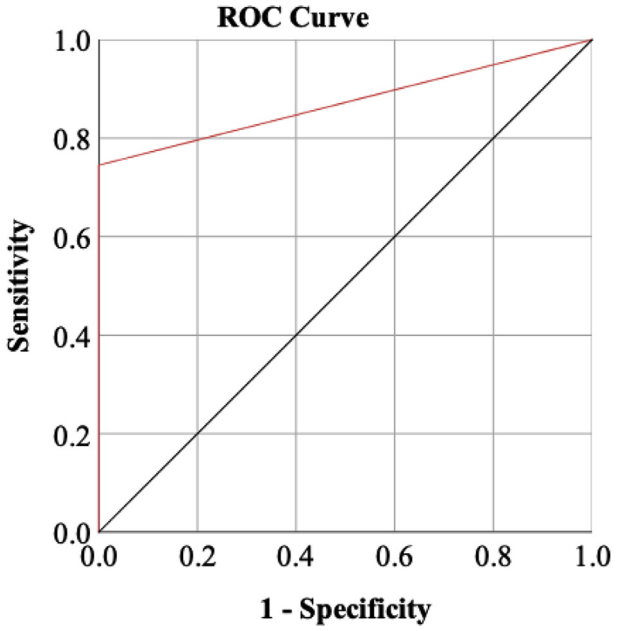

Fig. 4. **AUC of the model for the diagnosis of pituitary hypophysitis.** The ROC curve is represented in the overall population and reached similar performance in both the training set with AUC = 0.91 (0.82, 1.00), $P < 10^{-8}$, and in the validation set with AUC = 0.94 (0.80, 1.00), P = 0.001. AUC = area under a receiver operating characteristic curve; ROC = receiver operating characteristic.

commonly used in the evaluation of pituitary pathology were not included in our analysis because of their low quotation in the included articles.

We chose meta-analysis because it was the only way to collect enough data with a diagnosis of certainty. For patients with PM, we did not take into account the individual anti-oncologic treatments for two reasons: scarce data are available for PM in patients undergoing ICB therapy, and based on our experience, we do not believe that the imaging appearance of PM differs significantly across treatment types. Additionally, we have prospectively tested our algorithm on three patients at our institutions that presented with new pituitary lesions after ICB initiation, and a correct classification was observed for all (2HP, 1PM).

The radiologist plays a crucial role in the care of patients treated with ICB, and the evaluation of response to treatment is a great challenge in the context of atypical patterns of response and progression with drugs targeting the immune environment. The radiologist faces new pituitary lesions, whether it be on routine oncological follow-up imaging or the targeted investigation of new headaches, ante-pituitary insufficiency or diabetes insipidus. Misinterpretation of the appearance and therefore pathology can yield vastly different treatment pathways and potentially expose the patient to significant morbidity that might have otherwise been avoided. Symptomatic HP for instance may be treated with corticosteroids and temporary suspension of the ICB [15], while a suspected PM may lead to a change of therapeutic regimen, neurosurgical intervention or radiotherapy. Our imaging-based decisional algorithm aims to help both radiologists and oncologists make the right diagnosis for early and optimised management of pituitary anomalies in the growing population of patients undergoing immunotherapy.

Authorship contributions

A.M., L.D. and S.A. designed research, collected data, analysed data and have written the manuscript. All authors contributed to critical review, editing and approved the final content of the manuscript.

Conflict of interest statement

None declared.

Acknowledgements

The authors would like to thank all their colleagues from Gustave Roussy Comprehensive Cancer Center, as well as every member of the iTOX committee at Université Paris Sud. L Dercle work was funded by a grant from the Philanthropia Foundation, Geneva, Switzerland and the foundation Nuovo-Soldati.

References

[1] Keir ME, Butte MJ, Freeman GJ, Sharpe AH. PD-1 and its ligands in tolerance and immunity. Annu Rev Immunol 2008;26(1):677–704.
[2] Peggs KS, Quezada SA, Korman AJ, Allison JP. Principles and use of anti-CTLA4 antibody in human cancer immunotherapy. Curr Opin Immunol 2006;18(2):206–13.
[3] La-Beck NM, Jean GW, Huynh C, Alzghari SK, Lowe DB. Immune checkpoint inhibitors: new insights and current place in cancer therapy. Pharmacother J Hum Pharmacol Drug Ther 2015;35(10):963–76.
[4] Robert C, Long GV, Brady B, Dutriaux C, Maio M, Mortier L, et al. Nivolumab in previously untreated melanoma without BRAF mutation. N Engl J Med 2015;372(4):320–30.
[5] Hodi FS, O'Day SJ, McDermott DF, Weber RW, Sosman JA, Haanen JB, et al. Improved survival with ipilimumab in patients with metastatic melanoma. N Engl J Med 2010;363(8):711–23.
[6] Brahmer J, Reckamp KL, Baas P, Crinò L, Eberhardt WE, Poddubskaya E, et al. Nivolumab versus docetaxel in advanced squamous-cell non-small-cell lung cancer. N Engl J Med 2015;373(2):123–35.
[7] Garon EB, Rizvi NA, Hui R, Leighl N, Balmanoukian AS, Eder JP, et al. Pembrolizumab for the treatment of non–small-cell lung cancer. N Engl J Med 2015;372(21):2018–28.
[8] Motzer RJ, Escudier B, McDermott DF, George S, Hammers HJ, Srinivas S, et al. Nivolumab versus everolimus in advanced renal cell carcinoma. N Engl J Med 2015;373(19):1803–13.
[9] Bilgin B, Sendur MAN, Akıncı MB, Dede DŞ, Yalçın B. Targeting the PD-1 pathway: a new hope for gastrointestinal cancers. Curr Med Res Opin 2017;33(4):749–59.

[10] Ferris RL, Blumenschein G, Fayette J, Guigay J, Colevas AD, Licitra L, et al. Nivolumab for recurrent squamous-cell carcinoma of the head and neck. N Engl J Med 2016;375(19):1856–67.
[11] Tang J, Yu JX, Hubbard-Lucey VM, Neftelinov ST, Hodge JP, Lin Y. Trial watch: the clinical trial landscape for PD1/PDL1 immune checkpoint inhibitors. Nat Rev Drug Discov 2018;17:854–5.
[12] Dercle L, Seban R-D, Lazarovici J, Schwartz LH, Houot R, Ammari S, et al. 18F-FDG PET and CT scans detect new imaging patterns of response and progression in patients with hodgkin lymphoma treated by anti–programmed death 1 immune checkpoint inhibitor. J Nucl Med 2018;59(1):15–24.
[13] Dercle L, Ammari S, Seban R-D, Schwartz LH, Houot R, Labaied N, et al. Kinetics and nadir of responses to immune checkpoint blockade by anti-PD1 in patients with classical Hodgkin lymphoma. Eur J Cancer 2018;91:136–44.
[14] Turpin A, Michot J-M, Kempf E, Mazeron R, Dartigues P, Terroir M, et al. Le lymphome de Hodgkin : stratégies thérapeutiques actuelles et futures. Bull Cancer (Paris) 2018;105(1):81–98.
[15] Champiat S, Lambotte O, Barreau E, Belkhir R, Berdelou A, Carbonnel F, et al. Management of immune checkpoint blockade dysimmune toxicities: a collaborative position paper. Ann Oncol 2016;27(4):559–74.
[16] Michot J-M, Mazeron R, Dercle L, Ammari S, Canova C, Marabelle A, et al. Abscopal effect in a Hodgkin lymphoma patient treated by an anti-programmed death 1 antibody. Eur J Cancer 2016;66:91–4.
[17] Weber JS, Hodi FS, Wolchok JD, Topalian SL, Schadendorf D, Larkin J, et al. Safety profile of nivolumab monotherapy: a pooled analysis of patients with advanced melanoma. J Clin Oncol 2016;35(7):785–92.
[18] Mekki A, Dercle L, Lichtenstein P, Marabelle A, Michot JM, Lambotte O, et al. Detection of immune-related adverse events by medical imaging in patients treated with anti-programmed cell death 1. Eur J Cancer 2018;96:91–104.
[19] Kwak JJ, Tirumani SH, Van den Abbeele AD, Koo PJ, Jacene HA. Cancer immunotherapy: imaging assessment of novel treatment response patterns and immune-related adverse events. RadioGraphics 2015;35(2):424–37.
[20] Haanen JBJBaG, Carbonnel F, Robert C, Kerr KM, Peters S, Larkin J, et al. Management of toxicities from immunotherapy: ESMO Clinical Practice Guidelines for diagnosis, treatment and follow-up. Ann Oncol 2018;29(4):iv264–6.
[21] Cukier P, Santini FC, Scaranti M, Hoff AO. Endocrine side effects of cancer immunotherapy. Endocr Relat Cancer 2017;24(12):T331–47.
[22] Iwama S, Remigis AD, Callahan MK, Slovin SF, Wolchok JD, Caturegli P. Pituitary expression of CTLA-4 mediates hypophysitis secondary to administration of CTLA-4 blocking antibody. Sci Transl Med 2014;6(230). 230ra45-230ra45.
[23] Solinas C, Porcu M, De Silva P, Musi M, Aspeslagh S, Scartozzi M, et al. Cancer immunotherapy-associated hypophysitis. Semin Oncol 2018;45(3):181–6.
[24] Larkin J, Chiarion-Sileni V, Gonzalez R, Grob JJ, Cowey CL, Lao CD, et al. Combined nivolumab and ipilimumab or monotherapy in untreated melanoma. N Engl J Med 2015;373(1):23–34.
[25] Weber J, Mandala M, Del Vecchio M, Gogas HJ, Arance AM, Cowey CL, et al. Adjuvant nivolumab versus ipilimumab in resected stage III or IV melanoma. N Engl J Med 2017;377(19):1824–35.
[26] Max MB, Deck MDF, Rottenberg DA. Pituitary metastasis: incidence in cancer patients and clinical differentiation from pituitary adenoma. Neurology 1981;31(8). 998–998.
[27] Shamseer L, Moher D, Clarke M, Ghersi D, Liberati A, Petticrew M, et al. Preferred reporting items for systematic review and meta-analysis protocols (PRISMA-P) 2015: elaboration and explanation. BMJ 2015;349:g7647.
[28] Bonneville J-F, Bonneville F, Cattin F, Nagi S. MRI of the pituitary gland. Springer International Publishing; 2016. https://www.springer.com/gp/book/9783319290416. [Accessed 26 October 2018].
[29] Cheema A. Ipilimumab-induced secondary hypophysitis. Endocr Pract 2018;24(9). 854–854.
[30] van der Hiel B, Blank CU, Haanen JB, Stokkel MP. Detection of early onset of hypophysitis by 18f-fdg Pet-ct in a patient with advanced stage melanoma treated with ipilimumab. Clin Nucl Med 2013;38(4). https://insights.ovid.com/pubmed?pmid=23455528. [Accessed 4 November 2018].
[31] Blansfield JA, Beck KE, Tran K, Yang JC, Hughes MS, Kammula US, et al. Cytotoxic T-lymphocyte–associated antigen-4 blockage can induce autoimmune hypophysitis in patients with metastatic melanoma and renal cancer. J Immunother Hagerstown MD 1997 2005;28(6):593–8.
[32] Albarel F, Gaudy C, Castinetti F, Carré T, Morange I, Conte-Devolx B, et al. Long-term follow-up of ipilimumab-induced hypophysitis, a common adverse event of the anti-CTLA-4 antibody in melanoma. Eur J Endocrinol 2015;172(2):195–204.
[33] Araujo PB, Coelho MCA, Arruda M, Gadelha MR, Neto LV. Ipilimumab-induced hypophysitis: review of the literature. J Endocrinol Invest 2015;38(11):1159–66.
[34] Carpenter KJ, Murtagh RD, Lilienfeld H, Weber J, Murtagh FR. Ipilimumab-induced hypophysitis: MR imaging findings. Am J Neuroradiol 2009;30(9):1751–3.
[35] Chang L-S, Yialamas MA. Checkpoint inhibitor-associated hypophysitis. J Gen Intern Med 2018;33(1):125–7.
[36] Chodakiewitz Y, Brown S, Boxerman JL, Brody JM, Rogg JM. Ipilimumab treatment associated pituitary hypophysitis: clinical presentation and imaging diagnosis. Clin Neurol Neurosurg 2014;125:125–30.
[37] Dillard T, Yedinak CG, Alumkal J, Fleseriu M. Anti-CTLA-4 antibody therapy associated autoimmune hypophysitis: serious immune related adverse events across a spectrum of cancer subtypes. Pituitary 2010;13(1):29–38.
[38] Hassanzadeh B, DeSanto J, Kattah JC. Ipilimumab-induced adenohypophysitis and orbital apex syndrome: importance of early diagnosis and management. Neuro Ophthalmol 2017;42(3):176–81.
[39] Johnson DB, Mudigonda TV, Sosman JA. Melanoma and a headache. JAMA Oncol 2015;1(8):1167–8.
[40] Juszczak A, Gupta A, Karavitaki N, Middleton MR, Grossman AB. MECHANISMS IN ENDOCRINOLOGY: ipilimumab: a novel immunomodulating therapy causing autoimmune hypophysitis: a case report and review. Eur J Endocrinol 2012;167(1):1–5.
[41] Kaehler KC, Egberts F, Lorigan P, Hauschild A. Anti-ctla-4 therapy-related autoimmune hypophysitis in a melanoma patient. Melanoma Res 2009;19(5):333–4.
[42] Kanie K, Iguchi G, Bando H, Fujita Y, Odake Y, Yoshida K, et al. Two cases of atezolizumab-induced hypophysitis. J Endocr Soc 2017;2(1):91–5.
[43] Mahzari M, Liu D, Arnaout A, Lochnan H. Immune checkpoint inhibitor therapy associated hypophysitis. Clin Med Insights Endocrinol Diabetes 2015;8:21–8.
[44] Majchel D, Korytkowski MT. Anticytotoxic T-lymphocyte antigen-4 induced autoimmune hypophysitis: a case report and literature review. Case Rep Endocrinol 2015. https://www.hindawi.com/journals/crie/2015/570293/. [Accessed 4 November 2018].
[45] Marlier J, Cocquyt V, Brochez L, Van Belle S, Kruse V. Ipilimumab, not just another anti-cancer therapy: hypophysitis as side effect illustrated by four case-reports. Endocrine 2014;47(3):878–83.

[46] Gunawan F, George E, Roberts A. Combination immune checkpoint inhibitor therapy nivolumab and ipilimumab associated with multiple endocrinopathies. Endocrinol Diabetes Metab Case Rep 2018:2018https. https://www.ncbi.nlm.nih.gov/pmc/articles/PMC5830856/.
[47] Ohara N, Ohashi K, Fujisaki T, Oda C, Ikeda Y, Yoneoka Y, et al. Isolated adrenocorticotropin deficiency due to nivolumab-induced hypophysitis in a patient with advanced lung adenocarcinoma: a case report and literature review. Intern Med 2018; 57(4):527–35.
[48] Okano Y, Satoh T, Horiguchi K, Toyoda M, Osaki A, Matsumoto S, et al. Nivolumab-induced hypophysitis in a patient with advanced malignant melanoma. Endocr J 2016;63(10): 905–12.
[49] Valecha G, Pant M, Ibrahim U, Atallah JP. Immunotherapy-induced autoimmune hypophysitis. J Oncol Pharm Pract 2017; 1078155217727142.
[50] Wachsmann JW, Ganti R, Peng F. Immune-mediated disease in ipilimumab immunotherapy of melanoma with FDG PET-CT. Acad Radiol 2017;24(1):111–5.
[51] Wallace J, Krupa M, Brennan J, Mihlon F. Ipilimumab cystic hypophysitis mimicking metastatic melanoma. Radiol Case Rep 2018;13(3):740–2.
[52] Iqbal F, Choudhary N, Flanagan D. A case of pituitary hypophysitis following treatment with ipilimumab. BioScientifica; 2016. https://www.endocrine-abstracts.org/ea/0044/ea0044EP72. [Accessed 27 October 2018].
[53] Al-Aridi R, El Sibai K, Fu P, Khan M, Selman WR, Arafah BM. Clinical and biochemical characteristic features of metastatic cancer to the sella turcica: an analytical review. Pituitary 2014; 17(6):575–87.
[54] Dutta P, Bhansali A, Shah VN, Walia R, Bhadada SK, Paramjeet S, et al. Pituitary metastasis as a presenting manifestation of silent systemic malignancy: a retrospective analysis of four cases. Indian J Endocrinol Metab 2011;15(3):S242–5.
[55] Bhatoe HS, Badwal S, Dutta V, Kannan N. Pituitary metastasis from medullary carcinoma of thyroid: case report and review of literature. J Neuro Oncol 2008;89(1):63.
[56] Ersoy R, Topaloglu O, Aydin C, Dirikoc A, Cakir B. Pituitary metastasis of breast cancer confirmed by fluorine-18 fluorodeoxyglucose positron emission tomography: a case report. J Endocrinol Invest 2007;30(6):532–3.
[57] Fridley J, Adams G, Rao V, Patel A, Humphries W, Goodman C, et al. Small cell lung cancer metastasis in the pituitary gland presenting with seizures and headache. J Clin Neurosci 2011; 18(3):420–2.
[58] Goglia U, Ferone D, Sidoti M, Spaziante R, Dadati P, Ravetti JL, et al. Treatment of a pituitary metastasis from a neuroendocrine tumour: case report and literature review. Pituitary 2008;11(1):93–102.
[59] Gołkowski F, Trofimiuk M, Czepko R, Buziak-Bereza M, Łopatka P, Adamek D, et al. Two rare cases of pituitary metastases from breast and kidney cancers. Exp Clin Endocrinol Diabetes 2007;115(8):537–40.
[60] Gopan T, Toms SA, Prayson RA, Suh JH, Hamrahian AH, Weil RJ. Symptomatic pituitary metastases from renal cell carcinoma. Pituitary 2007;10(3):251–9.
[61] He W, Chen F, Dalm B, Kirby PA, Greenlee JDW. Metastatic involvement of the pituitary gland: a systematic review with pooled individual patient data analysis. Pituitary 2015;18(1): 159–68.
[62] Kam J, Kam J, Mann GB, Phillips C, Wentworth JM, King J, et al. Solitary pituitary metastasis from HER2-positive breast cancer. Asia Pac J Clin Oncol 2017;13(2):e181–4.
[63] Karamouzis MV, Melachrinou M, Fratzoglou M, Labropoulou-Karatza C, Kalofonos HP. Hepatocellular carcinoma metastasis in the pituitary gland: case report and review of the literature. J Neuro Oncol 2003;63(2):173–7.
[64] Ko J-C, Yang P-C, Huang T-S, Yeh K-H, Kuo S-H, Luh K-T. Panhypopituitarism caused by solitary parasellar metastasis from lung cancer. Chest 1994;105(3):951–3.
[65] Koshiyama H, Ohgaki K, Hida S, Takasu K, Yumitori K, Shimatsu A, et al. Metastatic renal cell carcinoma to the pituitary gland presenting with hypopituitarism. J Endocrinol Invest 1992; 15(9):677–81.
[66] Lin E-Y, Hsieh C-T, Lin C-S, Tsai T-H, Chiang Y-H. Keyhole surgery for isolated pituitary stalk metastatic tumors: a case report and review of the literature. Min - Minim Invasive Neurosurg. 2008;51(04):222–4.
[67] Masui K, Yonezawa T, Shinji Y, Nakano R, Miyamae S. Pituitary apoplexy caused by hemorrhage from pituitary metastatic melanoma: case report. Neurol Med Chir (Tokyo) 2013;53(10): 695–8.
[68] Ozturk MA, Eren OO, Sarikaya B, Aslan E, Oyan B. Pituitary metastasis of colon adenocarcinoma: a rare occurrence. J Gastrointest Cancer 2014;45(1):85–7.
[69] Peppa M, Papaxoinis G, Xiros N, Hadjidakis D, Raptis SA, Economopoulos T. Panhypopituitarism due to metastases to the hypothalamus and the pituitary resulting from primary breast cancer: a case report and review of the literature. Clin Breast Cancer 2009;9(4):E4–7.
[70] Piedra MP, Brown PD, Carpenter PC, Link MJ. Resolution of diabetes insipidus following gamma knife surgery for a solitary metastasis to the pituitary stalk: case report. J Neurosurg 2004; 101(6):1053–6.
[71] Riemenschneider MJ, Beseoglu K, Hänggi D, Reifenberger G. Prostate adenocarcinoma metastasis in the pituitary gland. Arch Neurol 2009;66(8). 1036–1036.
[72] Siqueira PFD, Mathez ALG, Pedretti DB, Abucham J. Pituitary metastasis of lung neuroendocrine carcinoma: case report and literature review. Arch Endocrinol Metab 2015;59(6):548–53.
[73] Williams MD, Asa SL, Fuller GN. Medullary thyroid carcinoma metastatic to the pituitary gland: an unusual site of metastasis. Ann Diagn Pathol 2008;12(3):199–203.
[74] Ratti M, Passalacqua R, Poli R, Betri E, Crispino M, Poli R, et al. Pituitary gland metastasis from rectal cancer: report of a case and literature review. SpringerPlus 2013;2(1):467.
[75] Stojanović M, Pekić S, Doknić M, Miljić D, Ćirić S, Diklić A, et al. What's in the image? Pituitary metastasis from papillary carcinoma of the thyroid: a case report and a comprehensive review of the literature. Eur Thyroid J 2013;1(4):277–84.
[76] Beckett DJ, Gama R, Wright J, Ferns GAA. Renal carcinoma presenting with adrenocortical insufficiency due to a pituitary metastasis. Ann Clin Biochem 1998;35(4):542–4.
[77] Moreno-Perez O, Peiró FM, López P, Boix A, Meoro A, Serna-Candel C, et al. An isolated pituitary metastasis as presentation of a differentiated hepatocellular carcinoma mimicking a non-functioning macroadenoma. J Endocrinol Invest 2007;30(5): 428–33.
[78] Agarwal KK, Sharma P, Singla S, Kc SS, Bal C, Kumar R. A rare case of non–small cell lung cancer metastasizing to the pituitary gland: detection with 18f-fdg Pet-ct. Clin Nucl Med 2014;39(5). https://insights.ovid.com/crossref?an=00003072-201405000-00028. [Accessed 4 November 2018].
[79] Barbaro D, Desogus N, Boni G. Pituitary metastasis of thyroid cancer. Endocrine 2013;43(3):485–93.
[80] Kurkjian C, Armor JF, Kamble R, Ozer H, Kharfan-Dabaja MA. Symptomatic metastases to the pituitary infundibulum resulting from primary breast cancer. Int J Clin Oncol 2005;10(3):191–4.
[81] Castle-Kirszbaum M, Goldschlager T, Ho B, Wang YY, King J. Twelve cases of pituitary metastasis: a case series and review of the literature. Pituitary 2018;21(5):463–73.
[82] Santarpia L, Gagel RF, Sherman SI, Sarlis NJ, Evans DB, Hoff AO. Diabetes insipidus and panhypopituitarism due to intrasellar metastasis from medullary thyroid cancer. Head Neck 2009;31(3):419–23.

[83] Wendel C, Campitiello M, Plastino F, Eid N, Hennequin L, Quetin P, et al. Pituitary metastasis from renal cell carcinoma: description of a case report. Am J Case Rep 2017;18:7–11.
[84] Feletti A, Marton E, Rossi S, Canal F, Longatti P, Billeci D. Pituitary metastasis of Merkel cell carcinoma. J Neuro Oncol 2010;97(2):295–9.
[85] Kim YH, Lee B jun, Lee KJ, Cho JH. A case of pituitary metastasis from breast cancer that presented as left visual disturbance. J Korean Neurosurg Soc 2012;51(2):94–7.
[86] Chu T-P, Tsai C-C, Chan W-C, Tzen C-Y, Chang Y-C. Solitary pituitary metastasis from breast cancer that presented as visual field defect. J Cancer Res Pract 2016;3(4):140–3.
[87] Kanayama S, Matsuno A, Nagashima T, Ishida Y. Symptomatic pituitary metastasis of malignant thymoma. J Clin Neurosci 2005; 12(8):953–6.
[88] Mota JS, de Sá Caldas A, de Araújo Cortês Nascimento AGP, dos Santos Faria M, Sobral CSP. Pituitary metastasis of thyroid carcinoma: a case report. Am J Case Rep 2018;19: 896–902.
[89] Rajput R, Bhansali A, Dutta P, Gupta SK, Radotra BD, Bhadada S. Pituitary metastasis masquerading as non-functioning pituitary adenoma in a woman with adenocarcinoma lung. Pituitary 2006;9(2):155–7.
[90] Bišof V, Juretić A, Šarić N, Melada A, Perković Z, Radoš M, et al. Pituitary metastasis of renal cell carcinoma : a case report. Radiol Oncol 2009;42(4):225–31.
[91] Hsiao C-H, Wang C-Y, Chung M-T, Yang M-S. Diabetes insipidus due to pituitary metastasis in a woman with lung adenocarcinoma: a case report. Cent Eur J Med 2011;6(4):475–9.
[92] Lim W, Lim DS, Chng CL, Lim AY. Thyroid carcinoma with pituitary metastases: 2 case reports and literature review. Case Rep Endocrinol 2015;2015. https://www.ncbi.nlm.nih.gov/pmc/articles/PMC4320791/.
[93] Eggermont AMM, Chiarion-Sileni V, Grob J-J, Dummer R, Wolchok JD, Schmidt H, et al. Adjuvant ipilimumab versus placebo after complete resection of high-risk stage III melanoma (EORTC 18071): a randomised, double-blind, phase 3 trial. Lancet Oncol 2015;16(5):522–30.
[94] Prete A, Salvatori R. Hypophysitis. In: De Groot LJ, Chrousos G, Dungan K, et al., editors. Endotext. South Dartmouth (MA): MDText.com, Inc.; 2018. http://www.ncbi.nlm.nih.gov/books/NBK519842/.